http://doi.org/10.36582/j.Alkuno.2025.11.02
Al-Kunooze University College
Journal homepage: http://journals.kunoozu.edu.iq/1/archive &
http:// www.iasj.net

Exploring The Potential of Copper Nanoparticles Against Gram-Positive and Gram-Negative Pathogenic Bacteria

Intisar Albandar[a]*

[a]*Department of Biology, College of Sciences, University of Basrah, Basrah, Iraq*

Abstract

Copper nanoparticles (CuNPs) are in urgent demand in the multi-drug-resistant bacteria (MDR) matter. In this context, this study sought to synthesize eco-friendly copper nanoparticles (CuNPs) and estimate their anti-bacterial ability against gram-positive and gram-negative multi-drug resistance bacteria to antibiotics. CuNPs were synthesized using an aqueous solution of copper sulfate $CuSO_4$ (100mM) with an aqueous leaf extract (3%) with a volume ratio of 1:1. The characterization of CuNPs was performed via an ultraviolet-visible spectrophotometer (UV-vis), zetasizer, zeta potential, scanning electron microscopy (SEM) and Fourier-transform infrared spectroscopy (FTIR). The antibacterial potential of CuNPs against Gram-positive (*S. haemolyticus*, *S. pneumonia*) and Gram-negative (*K. pneumonia* and *P. mirabilis*) pathogenic bacteria, was evaluated. The change of the mixture colour from light green to brown confirms CuNP synthesis. CuNPs demonstrated a Surface Plasmon Resonance (SPR) peak at 570 nm, with a size of 78.82 (d.nm) and 75-85 nm using zetasizer and SEM, respectively, with a semi-spherical shape. Zeta potential showed a value of -20.7mV and FTIR analysis revealed the biochemical compounds of plant extract. CuNPs illustrated remarkable antibacterial effectiveness with entire hemocompatibility with red blood cells. The antibacterial activity of CuNPs (200 µg/ml) showed inhibition zones of 20.00±1.00 mm, 17.66±0.66 mm, and 16.66±0.66 mm against *K. pneumonia*, *P. mirabilis*, and *S. haemolyticus*, respectively. Further, for the CuNPs at 50 and 100 µg/ml, the inhibition zones for *P. mirabilis* bacteria were 15.5±0.50 mm and 18.00±1.00 mm, respectively. Thus, CuNPs could be promisingly exploited to deter pathogenic bacteria with no recorded toxicity to human RBCs.

Keywords: Antibacterial, CuNPs, MDR, Nanoparticles, Nanotechnology, Resistant bacteria

1. Introduction

Nanotechnology has emerged as a viable solution for many health problems, such as multi-drug-resistant bacteria (MDR). The deficit of production of new generations of antibiotics through the last decades, incorporated with the disposition of pathogenic bacteria to evolve antibiotic resistance, show a grave worldwide hazard to human health [1]. Owing to the ability of pathogens to resist the available drugs, an alternative therapeutic procedure is required [2], which includes the need to discover new ones [3,4]. Further, the available drugs are exclusive to specific pathogens, thus, there is a driven demand to find sufficient medicine for newly emerged resistant strains [5].

Since copper is a common metal in different biomedical applications, it has currently been used for therapeutic purposes such as wound mending, and cancer radiotherapy, in addition to tumor imaging, immunological imaging [6]. Metal nanoparticles (MNPs) are adorable materials for scientific and applied research, which expanded rapidly nowadays. MNPs offer special properties including nano-sized scale, large surface area to volume ratio, clear stability, massive surface conditioning, and various shapes, which direct to an extensive range of applications [7,8].

Chemical, physical, and biological processes can fabricate the CuNPs. However, there is a rising demand for biological approaches due to their simplicity and eco-friendly properties compared to others [9]. CuNPs exhibit antimicrobial, antifungal, anti-cancer, and antioxidant, effects and deliver slight toxicity in comparison to other different MNPs [10]. CuNPs are deemed more unique subjects with valuable offers in different fields. They are broadly addressed as antimicrobial agents due to their tight interaction with bacterial membranes, leading to bacterial cell death. Further, CuNPs exhibit heightened catalytic activity by releasing copper ions in the solutions and, thus, can be utilized as electrochemical and biosensors [11-13].

Salvia officinalis (Sage) is a medicinal plant from the Lamiaceae family. It was originally grown in the Middle East but then has spread worldwide. This medicinal plant was selected due to its great proficiency against pathogens. It has been utilized to treat diverse illnesses including ulcers, seizures, rheumatism, diarrhea, gout, dizziness, inflammation, paralysis, tremor, and hyperglycemia [14,15]. The chemical compounds implicated presented in *S. officinalis* leaves' extract showed antibacterial impacts against different MDR bacteria such as vancomycin-resistant enterococci, penicillin-resistant *Streptococcus pneumonia*, and methicillin-resistant *Staphylococcus haemolyticus*, as well as *Enterococcus faecium* [16,17].

In this investigation, it was suggested to employ the aqueous leaf extract of *S. officinalis* to synthesize CuNPs by reducing the Cu^{+} ions to Cu^{0} form and using it to eliminate Gram-negative and Gram-positive bacteria.

2. Methods

2. 1. The materials and *Salvia officinalis* dry leaves

The materials used in this study are: Muller Hinton agar, Nutrient agar, Nutrient broth and Copper sulfate (99%) (Sigma Aldrich). Further, the pathogenic isolates used in this study are, *Staphylococcus haemolyticus* (urine culture), *Streptococcus pneumonia* (sputum culture), *Klebsiella pneumonia* (sputum culture) and *Proteus mirabilis* (stool culture). The isolates were collected from the laboratory of Al-Zubair General Hospital from different clinical sources, identified and tested for antibiotic resistance using Vitek 2 system (Healthcare, General Hospital of Al-Zubair). Dry leaves of *S. officinalis* were gathered from the local market at Basrah Governorate, Iraq. Leaves then were grinded using electric grinder (Brand Mart, Germany), and the powdered leaves were kept in tight containers at 4°C until use.

2. 2 Preparation of the aqueous extract of *Salvia officinalis* leaves

The aqueous extract of *S. officinalis* leaves was prepared using the protocol of [18]. Three grams of *S. officinalis* dried powder were added into 250 ml glass beaker, then 100 ml of distilled water was added and boiled for 10 min at 40-45 °C with continuously stirring using magnetic stirrer. The beaker was then left to cool down, and then the extract was filtered using a few layers of cotton and filter paper that were placed inside a funnel to get plant small parts-free extract. The extract was then stored at 4 °C for 2 weeks until used.

2. 3 Synthesis of Copper nanoparticles (CuNPs)

CuNPs were synthesized by mixing a freshly prepared aqueous extract of *S. officinalis* leaves with 100mM of copper sulfate at a ratio of (1:1) in a 250 ml glass flask. The mixture was then left on a magnetic stirring at 50-60 °C for 30 min then at room temperature (RT) for 24 hr. Next, the successful reduction of Cu ions to CuNPs was verified by observing the changing of the mixture colour from yellowish-green to brown after 48 hr of reaction. The obtained CuNPs were then centrifuged at 10,000 rpm for 15 minutes. The pellet was then collected and washed twice using sterile distilled water, and then dried in oven at 40 °C [19]. The schematic of study's design is displayed in Figure 1.

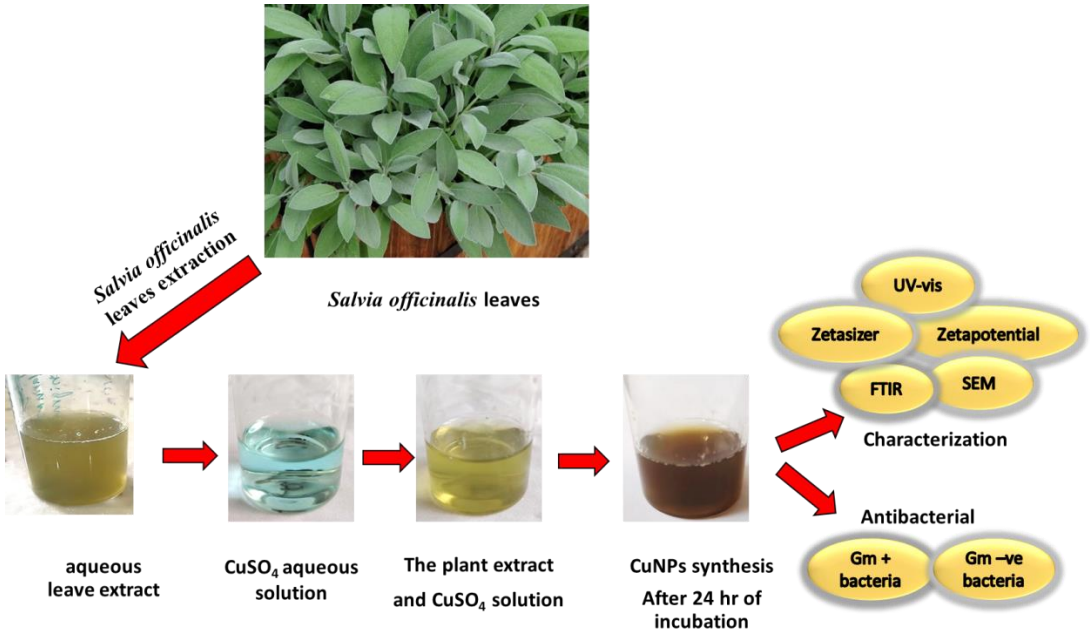

Fig. 1 - The schematic of study's design.

2. 4 Characterization of biogenic synthesized CuNPs

The CuNPs were confirmed by identifying the existence and the locality of Surface Plasmon resonance (SPR) peak via a UV–Vis spectroscopy between 350 nm and 800 nm. Malvern Zetasizer device (Nano ZS (v2.2)), was used to identify many parameters, such as Size of nanoparticles, Z-Average (d.nm), Number of nanoparticles (%), peak position, Intercept, Standard Deviation, and finally Result quality, which all validate the quality of CuNPs synthesis. A nano ZS instrument was used to investigate the Zeta potential value and identify the type of surface charge of CuNPs. The FTIR investigation of CuNPs was conducted employing FTIR device (BRUKER) at the region of the wavelengths ranging from 4000 to 400 cm^{-1}, to find the reducing chemical materials in the plant. Scanning electron microscope, NanoSEM^{TM} 450 (Nebraska Centre for Materials and Nanoscience) was used to take the images of the CuNPs, using a Low voltage 13.00 kV but getting high resolution.

2. 5 Hemocompatibility study of CuNPs with Red blood cells

A hemocompatibility test was managed to assess the cytotoxicity of CuNPs [20]. Ten ml of blood sample was gathered in anticoagulant tubes. Next, two ml of the above blood sample was separately transferred to five tubes, then washed using 4 ml of normal saline. The tubes were centrifuged for 10 min at 6,000 rpm, then the RBCs were collected at the bottom of the tubes, while the supernatant was discarded. Next, 2 ml of normal saline was added to the first tube as a negative control tube. Another 2 ml was mixed with 4 ml of Triton X as the positive control. Lastly, three different concentrations, 10, 20, and 40 µg\ ml of CuNPs prepared using normal saline were added to the last three tubes. All tubes were incubated for 60 min at RT and were centrifuged at 10,000 rpm for 5 min. The supernatant from each tube was collected and used to measure the absorbance at 495 nm operating enzyme-linked immunosorbent, ELISA, (800 TS microplate reader). The hemolysis rate % was considered using the formula [21, 22]:

$$\% \text{ Haemolysis } = \frac{\text{Mean OD of Sample} - \text{Mean OD of negative control}}{\text{Mean OD of positive control} - \text{Mean OD of negative control} \times 100} \quad (1)$$

2. 6 The Antibacterial activity of CuNPs

The antibacterial efficiency of CuNPs against Gram positive (*Staphylococcus haemolyticus*, *Streptococcus pneumonia*) and Gram negative (*Klebsiella pneumonia* and *Proteus mirabilis*) isolates was conducted via a well diffusion method [23]. Firstly, the isolates were tested for different types of antibiotics using Vitek test. To perform the well diffusion method, 100 µl of purified isolated bacteria, cultured for 18 hr in a nutrient broth, were spread on the surface of Muller Hinton agar plate. Next, three wells (6mm) were prepared in each plate. The wells were filled with 100 µl of Dimethyl sulfoxide (DMSO), which used as negative control, $CuSO_4$ salt, and CuNPs (50, 100 and 200 µg\ml), individually. The tested plates were aerobically incubated at 37°C for 24 hr. The clear inhibition zones around wells were determined after incubation time.

3. Results

3. 1 Synthesis of CuNPs

The color of the mixture (Fig. 2, A) was changed from light-green to brown (Fig. 2, B) after 24 hr of incubation at RT, which indicating the fast reduction of Copper ions of the aqueous solution into metallic copper. The metallic copper yielded as small crystals and eventually altered into colloidal CuNPs.

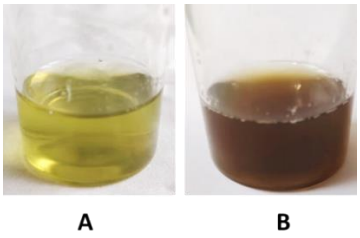

Fig. 2 - Synthesis of CuNPs: (A) The mixture of *S. officinalis* and $CuSO_4$ after 30 min of incubation at RT, and (B) The mixture of *S. officinalis* and $CuSO_4$ after 24 hr of incubation at 25°C.

3. 2 Characterisation of CuNPs

Fig. 3 displays the surface plasmon resonance peak of CuNPs using UV-vis absorption spectra. It can be seen that the absorption of CuNPs was located at the position of 570 nm.

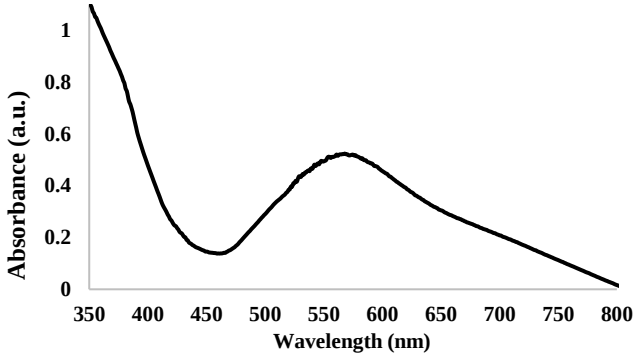

Fig. 3 - The absorbance of CuNPs with SPR peak using UV–vis spectrophotometer.

In the current study, FTIR was performed to explore the role of the chemical compounds in the plant extract in capping and stabilizing the CuNPs during the biosynthesis process. Fig. 4 presents FTIR bands with various wavelengths. The broad band at a wavelength of 3417.86 cm^{-1} is attributed to the existence of a hydroxyl bond O-H in alcoholic and phenolic compounds of the aqueous leaf extract. CuNPs' FTIR manifests two expected peaks at wavelengths of 2916.37 cm^{-1} and 2848.86 cm-1, in addition to the bands at 1635.64 cm^{-1} and 1436.97 cm^{-1}, which are attributed to the

aromatic compounds. Further, three other bands at 1261.45 cm^{-1}, 1165.00 cm^{-1} and 1026.13 cm^{-1} are stretching of the phenolic compounds of flavonoids. The two small bands at 798.53 cm^{-1} and 518.85 cm^{-1} correspond to reacting Cu ions with the organic compounds of the extract to produce bonds of Cu-O-H and Cu-O, respectively.

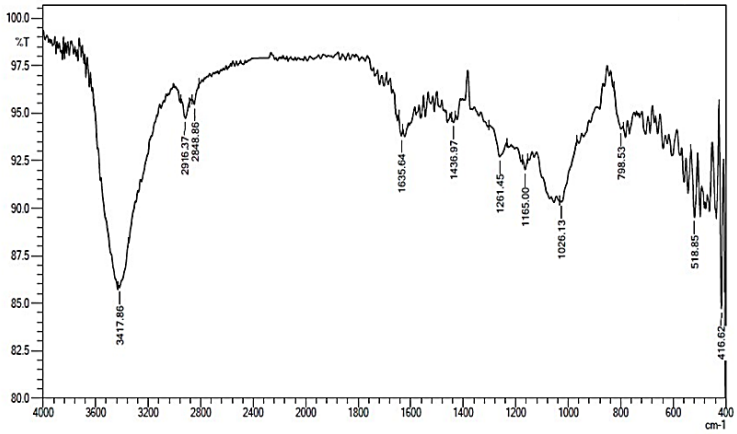

Fig. 4 - FTIR analysis of CuNPs using *Salvia officinalis* leaf extract.

The size distribution of CuNPs was acquired using the Zetasizer analysis with the Malvern Nano ZS instrument. CuNPs' size distribution is displayed in Fig. 5 and presents meaningful data. The analysis showed that the particle size of CuNPs was 78.82, the Z-Average (d.nm) was 195.4, Standard Deviation (8.445), and the sample quality (good). Moreover, a parameter of the Polydispersity index (PDI) of (0.9), indicates the monodispersed feature of CuNPs, which is induced from the distribution summary. The size distribution analysis information is shown in Table 1.

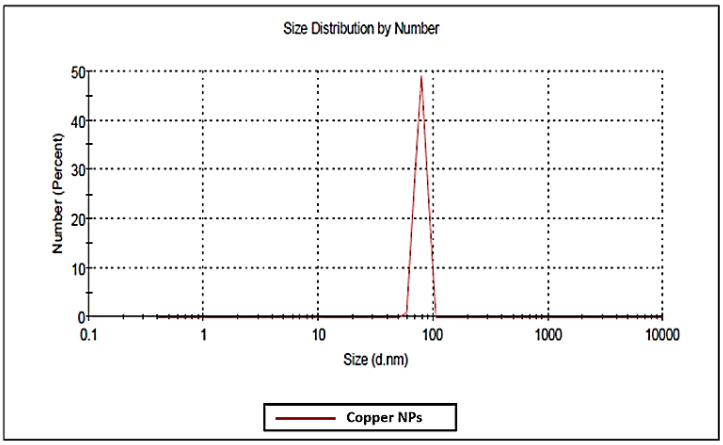

Fig. 5 - Size distribution analysis against the number of CuNPs.

Table 1 - Size distribution report of Zeta sizer analysis.

Parameter	Value
Z-Average (d.nm)	195.4
PDI	0.90
Size (d.nm)	78.82
% number	100
Standard Deviation	8.445
Intercept	1.01

Fig. 6 dictates the zeta potential of CuNPs (Zeta, Malvern panalytica, Malvern). The value of CuNPs zeta potential synthesized using *S. officinalis* was -20.7mV/ 100.0%.

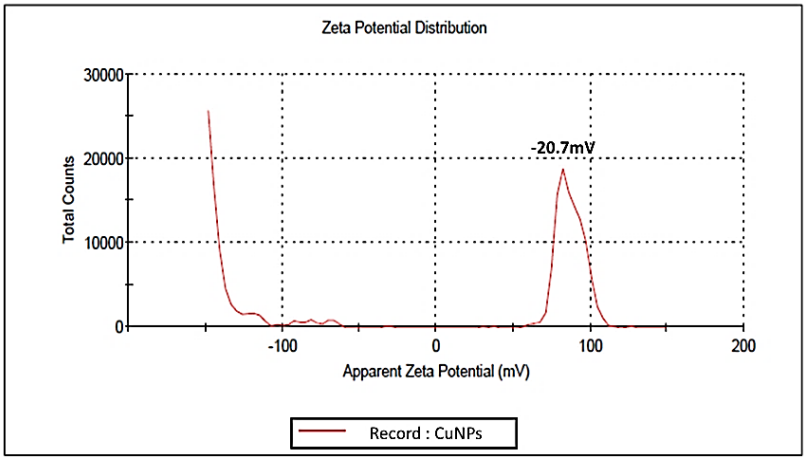

Fig. 6 - Zeta potential analysis of CuNPs.

SEM image investigation was performed in this study to gain visual pictures of CuNPs, as illustrated in Fig. 7. CuNPs showed monodispersed and semi-spherical shape using SEM analysis. The CuNPs exhibited a size of about 75-85 nm, with a homogenous distribution, in the absence of any evidence of aggregation.

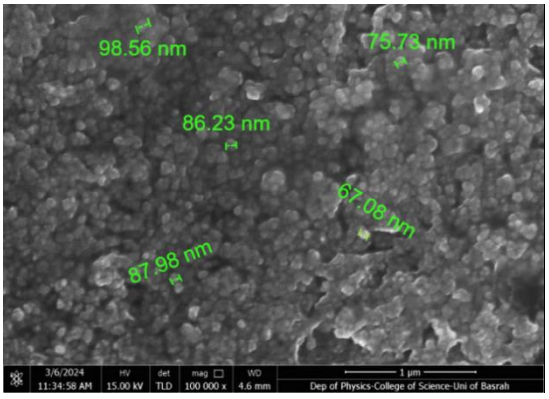

Fig. 7 - SEM of CuNPs.

3. 3 Hemocompatibility analysis of CuNPs

Fig. 8 demonstrates that the CuNPs showed no proof of RBC hemolysis after incubating with RBCs for 60 min at RT. The result showed that both CuNPs and normal saline had no RBC hemolysis activity, while Triton-X revealed 100% of the hemolysis in RBCs once mixed with RBCs.

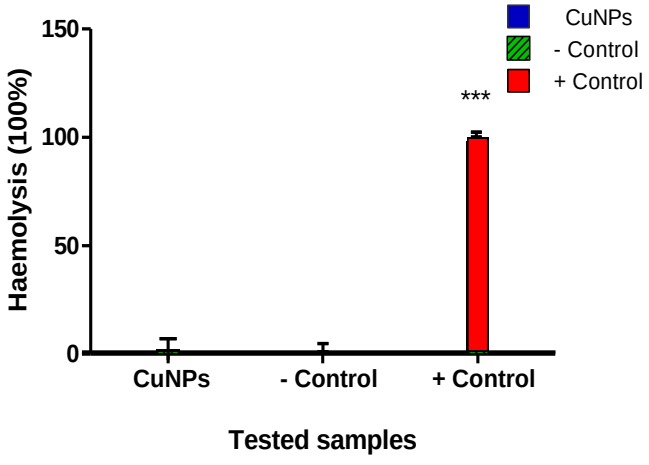

Fig. 8 - Hemocompatibility evaluation of CuNPs

3. 4 Antibacterial effectivness of CuNPs against Gr+ve and Gr-ve bacteria

The antibacterial efficacy of CuNPs was considered against four types of pathogenic bacteria, *S. haemolyticus* and *S. pneumonia* as Gram-positive, and *K. pneumonia* and *P. mirabilis* as Gram-negative bacteria. Moreover, the study was tested these bacteria to different types of standard antibiotics and found that the four types of bacteria were entirely resistant to at least five types of these standard antibiotics using the Vitek test, see Table 2.

Table 2 - Resistant bacteria to the different types of standard antibiotics using the Vitek test.

Resistant bacteria	**Standard antibiotics (MIC)* using Vitek test**				
S. haemolyticus	GEN	TOB	TET	OX	FUS
S. pneumonia	MOX	CLIN	BEN	ERY	LEV
K. pneumonia	AMP	CEF	CEFT	CIP	TRI
P. mirabilis	CEF	CEO	CEP	TIG	TRI

Resistance (R)

MIC=Minimum Inhibitory Concentration of antibiotics

GEN= Gentamycin 2, TOB= Tobramycin ≤ 1, TET= Tetracycline >8, OX= Oxacillin >2, FUS=Fusidic acid, MOX=Moxifloxacine 0.12, CLIN=Clindamycin>0.5, BEN=Benzylpenicillin>0.25, ERY=Erythromycin>160, LEV=Levofloxacin 4, AMP= Ampicillin >16, CEFT=Ceftazidime 32, CIP= Ciprofloxacin >2, TRI=Trimethoprim>160, CEF=Cefotaxime >32, CEO=Ceftolozane 16, CEP=Cefepime 16, TIG=Tigecycline 12, TRI=Trimethoprim>160 ,

The test of CuNPs against selected bacteria was applied using the agar well diffusion method by calculating the diameters of the inhibition areas around the wells prepared in Muller-Hinton media. The results revealed clear inhibition zones from the treatment with CuNPs and showed significant differences between the CuNPs and DMSO and $CuSO_4$ solution in the wells' diameters as shown in Fig. 9 and Table 3. The CuNPs with concentrations of 50, 100, and 200 µg\ml showed a gradual antibacterial impact on the chosen four types of pathogenic bacteria.

Further, the $CuSO_4$ solution did not affect bacteria, however, revealed small clear zones against *K. pneumonia*, which may indicate the sensitivity of this bacteria to $CuSO_4$. DMSO, which was used as a negative control, had no effect counter to all MDR isolates. Thus, CuNPs indicate the antibacterial activity when compared to the $CuSO_4$ solution, DMSO and antibiotics. The values of the inhibition zone means diameters of CuNPs shown in Table 3. In addition, Fig. 10 shows the mean of inhibition zones of CuNPs, $CuSO_4$ and DMSO.

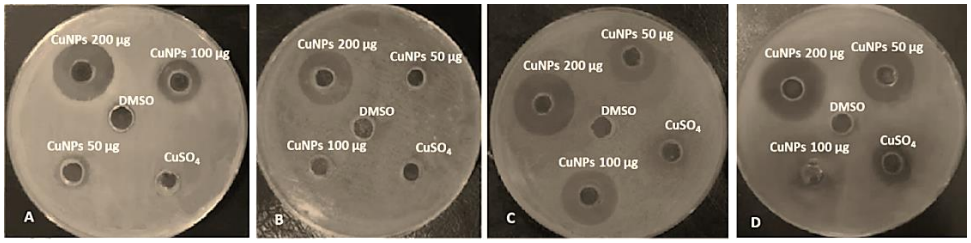

Fig. 9 - Antimicrobial activity of CuNPs that were used at various concentrations (50, 100, and 200 µg/ml) against MDR gram-positive and gram-negative bacteria, (A) *S. haemolyticus*, (B) *S. pneumonia*, (C) *K. pneumonia*, and (D) *P. mirabilis* as shown by the inhibition zones. Different antibiotics in VITEK test were used as positive controls, DMSO was used as negative control.

Table 3 - The inhibition zone diameters (mm) against MDR bacteria.

Bacterial isolates	Inhibition zones (mm)				
	DMSO*	$CuSO_4$ (100mM)	CuNPs (µg/ml) 50	100	200
S. haemolyticus	06.00±0.00	06.00±0.00	07.00±0.00*	10.33±0.66	16.66±0.66
S. pneumonia	06.00±0.00	06.00±0.00	05.80±0.60	06.00±0.00	15.33±0.66
K. pneumonia	06.00±0.00	06.00±0.00	09.66±0.66	16.66±0.66	20.00±1.00
P. mirabilis	06.33±0.33	08.00±0.00	15.5±0.50	18.00±1.00	17.66±0.66

*DMSO= *negative control*

*Represents the mean ± standard deviation (SD) of inhibition zones of three replicates

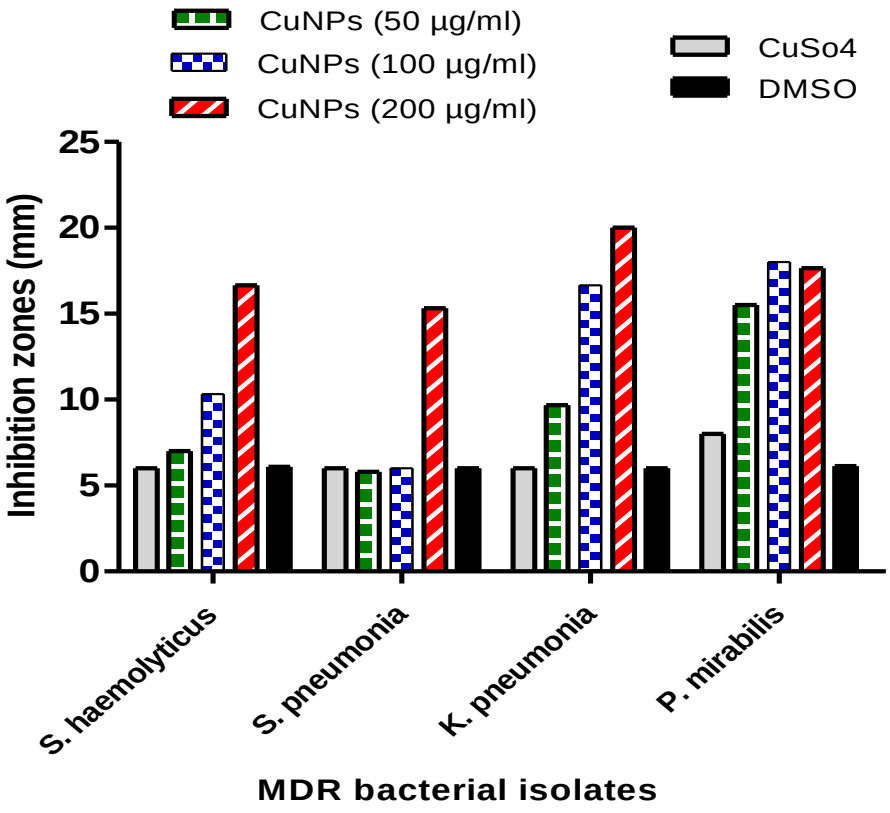

Fig. 10 - Mean of inhibition zones of different treatments CuNPs 50, 100, and 200 (µg/ml), $CuSO_4$ and DMSO against MRD bacteria *S. haemolyticus*, *S. pneumonia*, *K. pneumonia*, and *P. mirabilis*.

4. Discussion

Nanotechnology, an important branch of advanced science, has gained significant attention. Green synthesized nanoparticles using biological sources have gathered worldwide recognition compared to chemically synthesized ones, which are highly toxic and unfeasible [9]. The *S. officinalis* leaf extract contains diverse functional compounds such as ketones, tannins, proteins, polysaccharides, terpenoids, alkaloids, phenolic acid, vitamins and flavonoids [24]. It has been shown that these active

compounds are involved in potential nanoparticle synthesis [25]. Thus, this study proposes that the presence of these compounds contributes to the building of CuNPs.

The absorbance spectrum of CuNPs was recorded at 570 nm. This outcome conforms to the earlier studies that documented the absorption spectra of CuNPs at the range of 570 nm and at a range of 500-700 nm [26, 27]. It has been emphasized that UV-vis spectrometry is an approved strategy for nanoparticle characterization [28]. The appearance of the absorption peak at 570 nm, indicates the building of CuNPs due to the surface electrons that reveal a distinctive surface plasmon resonance. Furthermore, the absorption band can be used to expect the size of nanoparticles [29].

Moreover, by determining the positions of bonds, FTIR can specify the active chemical groups that are found on the CuNP surfaces [30]. Previous studies exhibited identical positions of bands from CuNPs using FTIR analysis. The band at a wavelength of 3417.86 cm-1, which resulted from the hydroxyl group O-H in alcoholic and phenolic compounds, might result from its adsorption on Cu ions in the time of CuNP capping during the synthesis process of CuNPs, which is accountable for the stability of CuNPs [31]. In addition, it has been demonstrated that the two bands at the wavelengths of 2916.37 cm^{-1} and 2848.86 cm^{-1} of CuNPs' FTIR, could be generated from the exchange of Cu ions with alcoholic or/ and phenolic active compounds and play a role in building and stabilizing CuNPs. Furthermore, the bands at 1635.64 cm^{-1} and 1436.97 cm^{-1} are related to C=O and C=C bonds of the aromatic compound present in the plant extract [32]. The bands at 1261.45 cm^{-1} and 1165.00 cm-1 were found to be related to phenolic compounds of flavonoids, while the band at 1026.13 cm^{-1} is related to the carbohydrates of the extract [33]. Moreover, the band at 798.53 cm^{-1} corresponds to methylene compounds in alkanes, while the band at 518.85 is responsible stretching of Cu-O [34]. In general, these conclusions confirm that active elements in the *S. officinalis* act to reduce Cu ions to synthesis of CuNPs [35]. The zeta sizer analysis was conducted to determine the size and the size distribution of CuNPs. This analysis is important to assess the quality of CuNPs by investigating their stability. A similar result of the zeta potential analysis was obtained for CuNPs in a study by Mohamed, (2020) by recording a size of 78 nm [36].

The zeta potential analysis is used to inquire into the surface charge of CuNPs, which play a role in the antibacterial activity of nanoparticles. It has been emphasised that the lowest value of zeta potential of ±30mV is wanted for stabilized nanoparticles [37]. The result of CuNP zeta potential (-20 mV) was found to be similar to the result of the study of [38]. The negative zeta potential value exhibited by the CuNPs could be a result of the possible capping of the organic biomolecules found in the *S. officinalis*

extract and indicates that the nanoparticles have unique stability features [39]. In the present study, it was confirmed that the biosynthesized CuNPs are not toxic materials using RBCs. Many studies have adopted this protocol due to its simplicity and time reduction compared to MTT assay using cell lines. The biocompatibility of CuNPs for RBCs in comparison to Triton-X was found to be similar to studies of [40, 41].

The antibacterial examination was conducted to assess the activity of the biosynthesized nanoparticles (CuNPs) in the eradication of MDR bacteria which showed resistance to five types of standard antibiotics. The outcomes concur with many studies revealing that the CuNPs exhibited antibacterial activity against Gram-positive and Gram-negative bacteria [42]. A present investigation emphasizes that the CuNPs exhibit high inhibitory impacts averse MDR bacteria. Further, our results are identical to many previous studies which indicated inhibitory activity from CuNPs against multi-drug resistant bacteria. It has been conveyed that free copper ions obstruct membrane porosity, which causes bacterial cell disturbance by leaking the cellular components [43]. A study disclosed that the antibacterial effect of the nanoparticles depends on the exciting release of reactive oxygen species (ROS) [44, 45]. The ROS are conducted for cell wall harm and disruption of respiratory chain enzymes, which lead to bacterial demise. The sensitivity of bacteria to the nanoparticles depends on the type of bacteria and type and the characterization of nanoparticles. Different types of metallic nanoparticles offer antibacterial activity against MDR bacteria [46], such as silver nanoparticles for MDR *S. aureus* and *E coli* [47], zinc oxide nanoparticles (ZnONPs) [48], iron oxide nanoparticles (MgONPs) for pathogenic bacteria [49], and selenium nanoparticles (SeNPs) for biofilm producer and Methicillin Resistant *Staphylococcus aureus* (MRSA) [50].

In general, our results contribute to investigating the importance of green synthesis for CuNPs, which includes reducing $CuSO_4$ by S. officinalis leaf extract. The characterization of CuNPs using four techniques validates the success of this method and is in line with previous studies by showing antibacterial efficiency.

5. Conclusion

The wide spectrum of CuNP applications is demanding investigators to inspect the significantly productive, eco-friendly, and cost-reasonable method for the synthesis of NPs. Fabrication of CuNPs was conducted using *S. officinalis* leaf aqueous extract,

which acts as a reducing agent to considerably enhance the CuNPs synthesis. Moreover, the promising sight of CuNPs occurred via the substantial antibacterial activity. Distinct effects of CuNPs were noticed against examined MDR bacteria including *S. haemolyticus*, *S. pneumonia*, *K. pneumonia*, and *P. mirabilis* compared to the standard antibiotics. Finally, since the green synthesized CuNPs hold numerous superiority over chemically synthesized nanoparticles by their obvious biocompatibility and are efficient against bacteria, it could be concluded that the CuNPs were valuable as antibacterial substances against MRD bacteria. Thus, this study imparts that these nanoparticles could be as alternates to antibiotics to reduce and control pathogens.

6. Acknowledgments

I wish to thank the Biology department/ College of Sciences/ University of Basrah to easiest performing the experiments at their labs. Likewise, my appreciation goes to the General Hospital of Al-Zubair for providing the bacterial isolates and all data related to VITEK 2 system (Healthcare, General Hospital of Al-Zubair).

7. References

1. Chin K, Michelle T, Luang-In V, Ma NL. An overview of antibiotic and antibiotic resistance. Environmental Advances 2022;11:100331.
2. Almkhadhree E, Alqaseer K, Radhi OA, Kadhim BA, Falah MA, Al-Yasseree H, Shnain WD, Albandar IJ, Shaker E. Community-Associated Methicillin-Resistant Staphylococcus aureus in the Oral Cavity. Kufa Journal for Nursing Sciences 2023;13:62-75.
3. Fisher MC, Alastruey-Izquierdo A, Berman J, Bicanic T, Bignell EM, Bowyer P, Bromley M, Brüggemann R, Garber G, Cornely OA, et al. Tackling the emerging threat of antifungal resistance to human health. Nature reviews Microbiology 2022;20:557-571.
4. Radhi O, Ali AH, Alqaseer, K, Shnain, WD, Albandar, IJ. Nosocomial Infections Associated with Caesarean Section. Kufa Journal for Nursing Sciences 2022;12(1).
5. Miethke M, Pieroni M, Weber T, Brönstrup M, Hammann P, Halby L, Arimondo PB, Glaser P, Aigle B, Bode HB, et al. Towards the sustainable discovery and development of new antibiotics. Nature reviews Chemistry 2021;5:726-749.
6. Wang P, Yuan Y, Xu K, Zhong H, Yang Y, Jin S, Yang K, Qi X. Biological applications of copper-containing materials. Bioactive materials 2021;6:916-927.
7. Khan M, Ullah H, Honey S, Talib Z, Abbas M, Ahmad T, Sohail J, Sohail A, Makgopa K, Ahmad J, et al. Metal Nanoparticles: Synthesis Approach Types and Applications – A Mini Review. Nano-Horizons 2023;2.

8. Albandar I, Jabbar S, Ibrahim TK, Radhi OA, Mbalaha ZS. Advances of Nanotechnology in Eradication Bacterial Infectious Diseases: A Recent Review. Kirkuk Journal of Science 2024;19;34-46.
9. Khan S, Shahid S, Sajid M, Noreen F, Kanwal S. Biogenic synthesis of CuO nanoparticles and their biomedical applications: a current review. International Journal of Advanced Research 2017;5:925-946.
10. Hasanin M, Al Abboud, MA, Alawlaqi, MM, Abdelghany, TM, Hashem, AH. Ecofriendly Synthesis of Biosynthesized Copper Nanoparticles with Starch-Based Nanocomposite: Antimicrobial, Antioxidant, and Anticancer Activities. Biological trace element research 2022;200:2099-2112.
11. Azizi-Lalabadi M, Garavand F, Jafari SM. Incorporation of silver nanoparticles into active antimicrobial nanocomposites: Release behavior, analyzing techniques, applications and safety issues. Advances in Colloid and Interface Science 2021;293:102440.
12. Wang Y, Cai B, Ni D, Sun Y, Wang G, Jiang H. A novel antibacterial and antifouling nanocomposite coated endotracheal tube to prevent ventilator-associated pneumonia. Journal of Nanobiotechnology 2022;20:112.
13. Keshari AK, Srivastava R, Singh P, Yadav VB, Nath G. Antioxidant and antibacterial activity of silver nanoparticles synthesized by Cestrum nocturnum. Journal of Ayurveda and integrative medicine 2020;11:37-44.
14. Ghorbani A, Esmaeilizadeh M. Pharmacological properties of Salvia officinalis and its components. Journal of traditional and complementary medicine 2017;7:433-440.
15. Jažo Z Glumac M Paštar V Bektić S Radan M Carev I. Chemical composition and biological activity of salvia officinalis L. Essential oil' Plants 2023;12:1794.
16. Mendes F, Garcia L, da Silva Moraes T, Casemiro L, de Alcântara C, Ambrósio S, Veneziani R, Miranda M, Martins C. Antibacterial activity of salvia officinalis L. against periodontopathogens: An in vitro study. Anaerobe 2020; 63:102194.
17. Lahlou Y, Moujabbir S, Aboukhalaf A, Amraoui BE, Bamhaoud T. Antibacterial activity of essential oils of Salvia Officinalis growing in Morocco. Roczniki Państwowego Zakładu Higieny/ Annals of the National Institute of Hygiene 2023;74:459-468.
18. Cavazos P, Gonzalez D, Lanorio J, Ynalvez R. Secondary metabolites antibacterial and antioxidant properties of the leaf extracts of Acacia rigidula benth and Acacia berlandieri benth. SN Applied Sciences 2021;3.
19. Shiravand S, Mahmoudvand H, Ebrahimi K. Biosynthesis of copper nanoparticles using aqueous extract of Capparis spinosa fruit and investigation of its antibacterial activity. Marmara Pharmaceutical Journal 2017;21:866-871.

20. Yedgar S, Barshtein G, Gural A. Hemolytic Activity of Nanoparticles as a Marker of Their Hemocompatibility. Micromachines 2022 13.
21. Sæb IP, Bjørås M, Franzyk H, Helgesen E, Booth JA. Optimization of the Hemolysis Assay for the Assessment of Cytotoxicity. International Journal of Molecular Science 2023;24:2914.
22. Bai J, Zhang M, Shao L, Jones TP, Feng X, Huang M, BéruBé K A. Hemolytic Properties of Fine Particulate Matter (PM2.5) in In Vitro Systems Toxics 2024;27:246.
23. Hossain ML, Lim LY, Hammer K, Hettiarachchi D, Locher CA. Review of Commonly Used Methodologies for Assessing the Antibacterial Activity of Honey and Honey Products. Antibiotics 2022;11:975.
24. Antonio-Pérez A, Durán-Armenta, LF, Pérez-Loredo, MG, Torres-Huerta, AL. Biosynthesis of Copper Nanoparticles with Medicinal Plants Extracts: From Extraction Methods to Applications. Micromachines 2023;14:1882.
25. Ullah, N, Ullah, A, Rasheed, S. Green synthesis of copper nanoparticles using extract of Dicliptera Roxburghiana, their characterization and photocatalytic activity against methylene blue degradation. Letters in Applied NanoBioScience 2020; 9: 897-901
26. Jeyaraman J, Jeyasubramanian K, Marikani A, Rajakumar G, Rahuman A, Thirunavukkarasu S, Arivarasan VK, Chidambaram J, Marimuthu S. Copper nanoparticles synthesized by polyol process used to control hematophagous parasites. Parasitology research 2011;109:1403-1415.
27. Amjad R, Mubeen B, Ali SS, Imam SS, Alshehri S, Ghoneim MM, Alzarea SI, Rasool R, Ullah I, Nadeem MS, et al. Green Synthesis and Characterization of Copper Nanoparticles Using Fortunella margarita Leaves. Polymers. 2021; 13(24):4364.
28. Quevedo AC Guggenheim E Briffa SM Adams J Lofts S Kwak M Lee TG Johnston C Wagner S Holbrook TR Hachenberger YU Tentschert J Davidson N Valsami-Jones E. UV-Vis Spectroscopic Characterization of Nanomaterials in Aqueous Media. J Vis Exp. 2021;25:176.
29. Henglein A. Formation and Absorption Spectrum of Copper Nanoparticles from the Radiolytic Reduction of Cu(CN)2. The Journal of Physical Chemistry B 2000;104:1206-1211.
30. Mekonnen KD. Fourier transform infrared spectroscopy as a tool for identifying the unique characteristic bands of lipid**s** in oilseed components: Confirmed via Ethiopian indigenous desert date fruit. Heliyon 2023;9:e14699.
31. Illakkia R, Mahesh N, Balakumar S, Sivakumar N, Kavitha Shree GG, Prem Rajan A, Govindasamy C, Aravind J. Adroit effect of copper nanoparticles and copper

nanozyme and their effective decolorization of azo dyes. Journal of King Saud University - Science 2024;36:103353.

32. Pelin I, Silion M, Popescu I, Rîmbu C, Fundueanu G, Constantin M. Pullulan/ Poly (vinyl alcohol) Hydrogels Loaded with Calendula officinalis Extract: Design and In Vitro Evaluation for Wound Healing Applications. Pharmaceutics 2023;15:1674.
33. Klink MJ, Laloo N, Leudjo Taka A, Pakade VE, Monapathi ME, Modise JS. Synthesis characterization and antimicrobial activity of zinc oxide nanoparticles against selected waterborne bacterial and yeast pathogens. Molecules 2022;27:3532.
34. Amaliyah S, Pangesti DP, Masruri M, Sabarudin A, Sumitro SB. Green synthesis and characterization of copper nanoparticles using Piper retrofractum Vahl extract as bioreductor and capping agent. Heliyon 2020;6:e04636.
35. Amjad R, Mubeen B, Ali SS, Imam SS, Alshehri S, Ghoneim MM, Alzarea SI, Rasool R, Ullah I, Nadeem MS, Kazmi I. Green Synthesis and Characterization of Copper Nanoparticles Using Fortunella margarita Leaves. Polymers (Basel) 2021;13:4364.
36. Mohamed EA Green synthesis of copper and copper oxide nanoparticles using the extract of seedless dates. Heliyon 2020;6:e03123.
37. León A, Plasencia J, Duran A, Albores A. Comparison of the In Vitro Antifungal and Anti-fumonigenic Activities of Copper and Silver Nanoparticles Against Fusarium verticillioides. Journal of Cluster Science, 2020;31:213-220.
38. Amir M, Butt RA, Hasany SF, Ahmed K. Non-Covalent Bonding of Green Synthesized Copper Nanoparticles to Enhance Physicochemical Behavior of Sulfur-Dyed Cotton Fabric. AATCC Journal of Research. 2023;10:280-288.
39. Narayanan V, Kathirason S, Elango P, Subramanian R, Sivagurusundar R, Gurusamy, A. Emilia sonchifolia leaf extract-mediated green synthesis, characterization, in vitro biological activities, photocatalytic degradation and in vivo Danio rerio embryo toxicity of copper nanoparticles. RSC Advances, 2023;13:16724-16740.
40. Attia AM, El-Banna SG, el-trass E, Yahya R, Azab A, Jbireal J, Shkal K Hematotoxicity Induced by Copper Oxide and/or Zinc Oxide Nanoparticles in Male Albino Rats. Journal of Biotechnology 2019;3:1-7.
41. Luu NH, Nguyen MN, Dang LH, Le TP, Doan TL, Nguyen TT, Le HK, Nguyen MT, Hoang LS, Tran NQ Antibacterial and biocompatible wound dressing based on green-synthesized copper nanoparticles and alginate. Journal of Materials Research 2024;39:955-967.

42. Ma X, Zhou S, Xu X, Du Q. Copper-containing nanoparticles: Mechanism of antimicrobial effect and application in dentistry-a narrative review. Front Surg. 2022;59:905892.
43. Raffi M, Mehrwan S, Bhatti TM. Investigations into the antibacterial behavior of copper nanoparticles against Escherichia coli. Annals of Microbiology 2010;60:75-80.
44. Mao BH, Chen ZY, Wang YJ, Yan SJ. Silver nanoparticles have lethal and sublethal adverse effects on development and longevity by inducing ROS-mediated stress responses. Scientific reports 2018;8:2445.
45. Nie P, Zhao Y, Xu H. Synthesis applications toxicity and toxicity mechanisms of silver nanoparticles: A review Ecotoxicology and Environmental Safety 2023;253:114636.
46. Mba IE, Nweze EI. Nanoparticles as therapeutic options for treating multidrug-resistant bacteria: research progress challenges and prospects. World journal of microbiology & biotechnology 2021;37:108.
47. Albandar I, Radhi OA, Al-Saadi SAM, Mahdi MA. Eco-Friendly Synthesis of Silver Nanoparticles Using Prosopis farcta Fruit Extract and Evaluate Their Biological Applications. Pakistan Journal of Life and Social Sciences 2024;1:3653-3665.
48. Tamanna I, Pitchiah S, Suresh V, Ramasamy P. Synthesis of Zinc Oxide Nanoparticles From Aqueous Extract of Avicennia marina Mangrove Leaves and Their Antibacterial Activities Against Oral Pathogens. Cureus 2023;15:e47627.
49. Yassin, MT, Al-Otibi, FO, Al–Askar, AA. Green synthesis, characterization and antimicrobial activity of iron oxide nanoparticles with tigecycline against multidrug resistant bacterial strains. Journal of King Saud University - Science 2024;36:103131.
50. Radhi O, Albandar I, Alqaseer K, Shnain W. Selenium nanoparticles inhibit Staphylococcus aureus-induced nosocomial infection cell death and biofilm formation. Journal of Population Therapeutics and Clinical Pharmacology 2023;30:367-378.